HIGH FILL-FACTOR TWO-AXIS ANALOG MICROMIRROR ARRAY FOR 1xN^2 WAVELENGTH-SELECTIVE SWITCHES

Jui-che Tsai, Sophia Huang, and Ming C. Wu
Electrical Engineering Department, University of California, Los Angeles
Los Angeles, CA 90095-1594, U.S.A.
TEL: 1-310-825-7338, FAX: 1-310-794-5513
E-mail: *jctsai@icsl.ucla.edu*

ABSTRACT

We report on a two-axis analog micromirror array with high fill factor (96%) and large mechanical scan angles (±4.4° and ±3.4°). To our knowledge, this is the highest linear fill factor ever reported for two-axis analog micromirror arrays. A 1x14 wavelength-selective switch (WSS) was also demonstrated using the mirror array. This is the largest number of port count ever reported for WSS. The fiber-to-fiber insertion loss is 8.2 dB. Switching of < 2 msec has been achieved.

INTRODUCTION

Micro-electro-mechanical mirrors are key enabling components for many wavelength-division-multiplexing (WDM) functions. They offer low optical insertion loss and low crosstalk, independence of polarization and wavelength, as well as optical transparency for bit rate and data format. Examples include 2D [1, 2] and 3D [3] MEMS optical switches, dynamic gain equalizers [4], wavelength add-drop multiplexers (WADM) [5], and wavelength-selective switches (WSS) [6-8].

Multi-port WSS, or 1xN WSS, has attracted a great deal of attention due to its routing capability. It combines wavelength demultiplexing, 1xN switching, and wavelength re-multiplexing functions in a very compact module. It is also the basic building block for NxN wavelength-selective crossconnect [7]. The maximum port count of the reported 1xN WSS is 4, which is limited by optical diffraction. Previously, we proposed and demonstrated a 1xN^2 WSS with a 2D collimator array [9-11]. The number of port count was increased from N to N^2. 2D beam steering was accomplished by using two separate one-dimensional arrays of one-axis micromirrors with orthogonal scanning directions in a *4-f confocal system*. A 1x8 WSS (using a 3x3 array of discrete collimators) has been achieved [10]. However, only half of the optical aperture is usable in the *4-f* confocal system. Furthermore, the *4-f* architecture requires more optical alignment.

The optical system can be simplified by using a high fill-factor two-axis analog micromirror array. More importantly, the port count can be doubled by fully utilizing the whole lens area. 2D beam steering is accomplished by the two-axis MEMS scanners, instead of cascaded one-axis micromirrors. Previous work on two-axis mircomirror arrays has been published [12]. However, their fill factor is too low (35%) for WSS applications. High fill-factor tip/tilt micromirror arrays for adaptive optics have also been reported [13]. However, the mirror tilt angle is relatively small (0.65°). In this paper, we report on a two-axis analog micromirror array with high fill factor (96%), achieved by hiding the springs and actuators underneath the mirrors. Large mechanical scan angles (±4.4° and ±3.4°) have been achieved. A 1x14 WSS was also constructed using the mirror array. The channel spacing is 50 GHz, and the fiber-to-fiber insertion is 8.2 dB.

TWO-AXIS ANALOG MICROMIRROR ARRAY

Gimbaled structures have been widely used in two-axis MEMS scanners [12]. However, the gimbals occupy large areas and sacrifice fill factor of the mirrors. Previously, an electroplated two-axis scanner with a crossbar torsion spring was proposed [14]. The crossbar torsion spring eliminates the need of gimbaled structures and is suitable for high-fill factor mirror arrays.

Figure 1 shows the schematic of the two-axis micromirror. Crossbar torsion springs hidden underneath the mirror are employed to achieve high fill factor. Four terraced electrodes [15] are employed to reduce the actuation voltage. The devices are fabricated using the SUMMiT-V surface micromachining process provided by Sandia National Laboratory. It has five polysilicon layers, including one nonreleasable ground layer (mmpoly0) and four structural layers (mmpoly1 to mmpoly4).

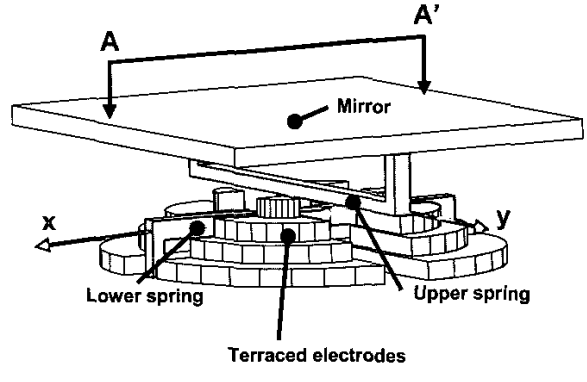

Figure 1. *Schematic of the two-axis analog micromirror with terraced electrodes and hidden crossbar torsion springs.*

0-7803-8265-X/04/$17.00 ©2004 IEEE.

Figure 2(a) shows the cross section of the two-axis analog micromirror and the corresponding polysilicon layers. The terraced electrodes are made of the bottom four polysilicon layers (mmpoly0 to mmpoly3), whereas the top polysilicon layer (mmpoly4) is designated for the mirror. The chemical-mechanical-planarization (CMP) process before the deposit of the top two polysilicon layers eliminates the topography underneath the mirrors, and provides a 10.75 μm gap between the mirror and substrate for rotation. Figure 2(b) shows the cross section of the mirror and the springs (along A-A' in Figure 1). For clarity, the terrace electrodes are not shown in this drawing. The crossbar torsion springs are composed of two parts. The lower spring (rotation about x axis) is made of stacked mmpoly1/mmpoly2 layers, while the upper spring (rotation about y axis) is made of mmpoly3 layer. This unique multilayer design enables us to achieve large clearance for *both* rotation axes: 6.5 μm and 6.25 μm for rotation about the lower (x axis) and upper (y axis) springs, respectively.

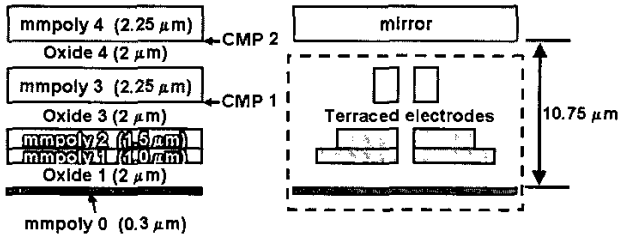

(a)

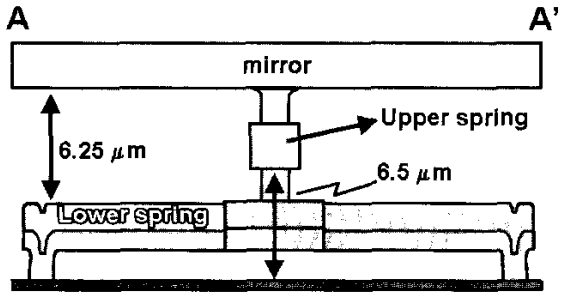

(b)

Figure 2. *(a) Cross section of the two-axis analog micromirror and the corresponding polysilicon layers in SUMMiT-V process, and (b) cross section of the mirror and the crossbar springs.(The electrodes are not shown in this figure).*

Figure 3(a) shows the scanning electron micrographs (SEM) of the two-axis micromirror. The lower half of the mirror is removed to reveal the underlying structures. The SEM of the array is shown in Figure 3(b). A high fill factor of 96% is achieved (96 μm mirror on 100 μm pitch). This is the highest fill factor ever reported for linear arrays of two-axis micromirrors. The array size is 1x10, limited by the chip size offered by the SUMMiT-V process. Figure 4 shows the DC scanning characteristics. Maximum scan angles of ±4.4° (at 90V) and ±3.4° (at 91.5V) are achieved. The mirror and the springs are grounded during actuation, whereas the electrodes are biased at the desired voltage. The difference in the actuation voltages for the two axes is due to the unequal spring constants for the lower spring and upper spring.

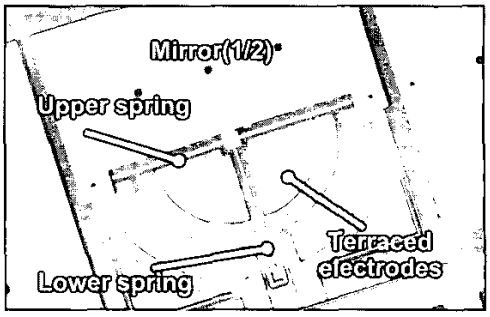

(a)

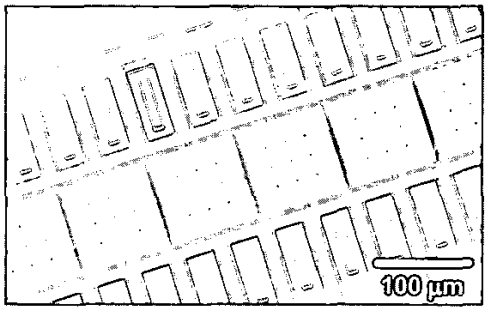

(b)

Figure 3. *SEM of (a) two-axis micromirror with the lower half of the mirror intentionally removed, and (b) 1x10 array of two-axis micromirrors.*

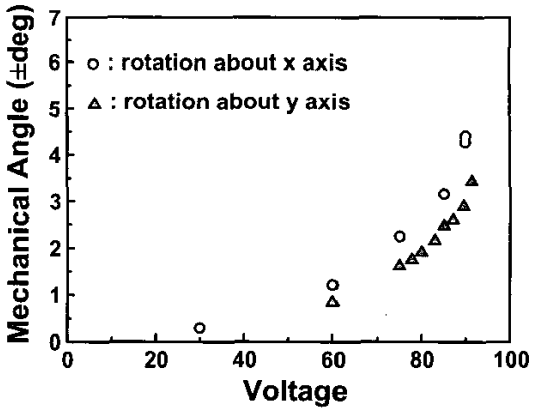

Figure 4. *DC characteristics of the two-axis micromirror: ±4.4° at 90V about x axis, and ±3.4° at 91.5V about y axis are achieved.*

Figure 5 shows the frequency responses of the two-axis scanner for both x and y axes. The resonant frequencies are 20.7 KHz and 24.3 KHz, respectively.

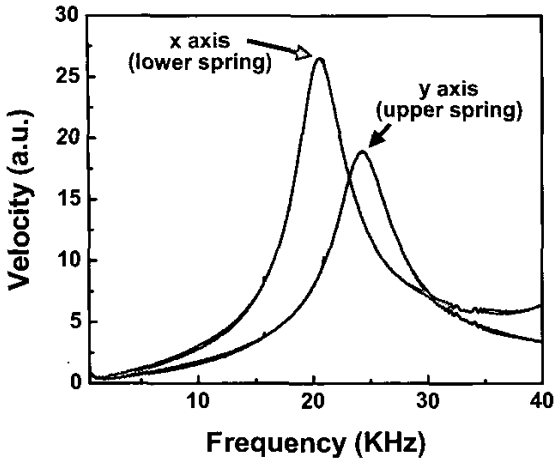

Figure 5. *Frequency responses of the two-axis MEMS mirror for both x and y axes. The resonant frequencies are 20.7 KHz and 24.3 KHz, respectively.*

1xN^2 Wavelength-Selective Switches

Figure 6 shows the schematic of the 1xN^2 WSS using the two-axis micromirror array. The center fiber of the 2D collimator array functions as the input, with the other ports serving as outputs. The WDM signals (wavelength channels) emerging from the input fiber are spatially dispersed by a diffraction grating, and focused onto its corresponding micromirror by the focusing lens. The two-axis mirrors direct individual wavelength signals to any arbitrary output port in the 2D collimator array, depending on the tilting directions and angles.

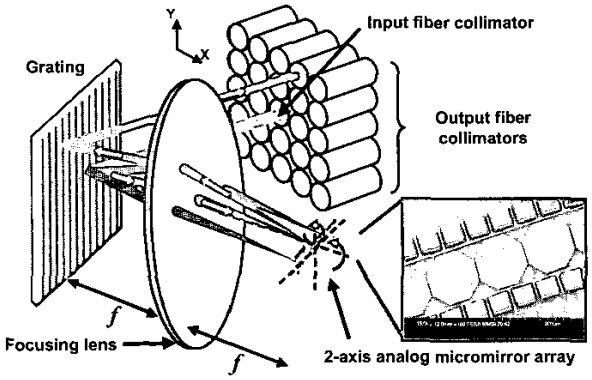

Figure 6. *Schematic setup of the 1xN^2 wavelength-selective switch. The inset shows the SEM picture of the two-axis micromirror array used in the optical system. The corners of the mirrors are cut to prevent physical contact between the mirror and the substrate during diagonal rotation.*

We have constructed a prototype system using an 1100-grooves/mm grating. The focal length of the lens is 30 cm. A channel spacing of 50 GHz has been achieved. The 1x10 micromirror array used is the WSS (shown in the inset of Figure 6) has a slightly different design. It has a larger pitch (200 μm) and a higher fill factor (98%). The scan angles are ±2.63° (at 14.1V) and ±1.27° (at 21.1V), for rotation about x and y axes, respectively. The rotational angles are smaller due to sagging resulting from softer springs. The corners of the mirrors are cut to prevent physical contact between the mirror and the substrate during diagonal rotation. The optical system supports a 3x5 array of discrete collimators. It functions as a 1x14 WSS with the center fiber collimator as the input port. This is the WSS with the largest port count ever reported. The number of ports in y direction is smaller due to the smaller scan angle in that direction.

The spectral responses for the 10 wavelength channels are shown in Figure 7. Spectra are measured at both the input port and the corner output port. Figure 7(a) shows the spectra when all wavelengths are coupled back to the input collimator. The ripples around 1548.1 nm and 1549.2 nm are due to mirrors experiencing pull-in during test. In Figure 7(b), the 1550-nm channel is switched to the corner output collimator. The optical insertion loss is 8.2 dB when the signal is coupled back to the input port. When coupled to the corner output port, the insertion loss is 15.9 dB. The insertion loss can be further optimized by improving the optical alignment. Figure 8 is the temporal response when the signal is switched to the output port. The switching time is < 2 msec.

Conclusion

We have reported on a two-axis analog micromirror array with high fill factor (96%) and large mechanical scan angles (±4.4° and ±3.4°). The high fill factor is achieved by hidden springs and electrodes. Terraced electrodes are employed to reduce the actuation voltage. A 1x14 wavelength-selective switch (WSS) has also been demonstrated using the two-axis MEMS mirror array. The channel spacing is 50 GHz, and the fiber-to-fiber insertion loss is measured to be 8.2 dB. Switching of < 2 msec has also been achieved

Acknowledgement

This project is supported by DARPA/SPAWAR under contract N66001-00-C-8088. The authors would like to thank Professor Joe Ford at University of California, San Diego for helpful discussions, and Dr. Dooyoung Hah of ETRI (South Korea), Ming-Chang Lee and Josh Chi of UCLA for SEM images and technical assistance.

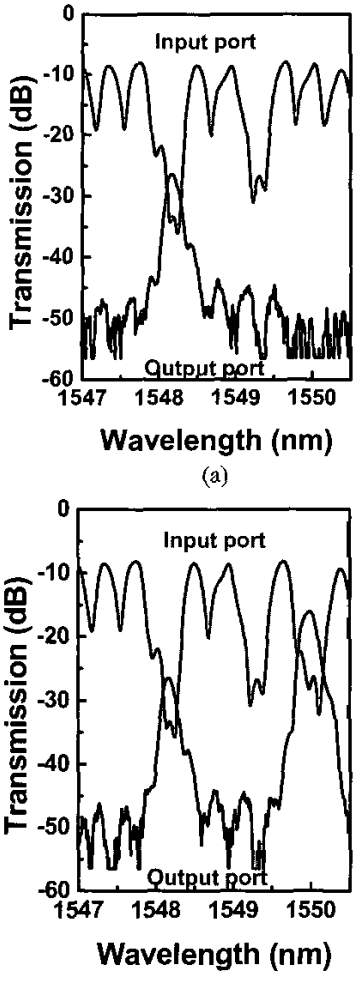

Figure 7. *Spectral response when (a) all channels coupled back to the input port, and (b) the 1550-nm channel is switched to the corner output port. The ripples at 1548.1 nm and 1549.2 nm are due to mirrors that experiences pull-in during test.*

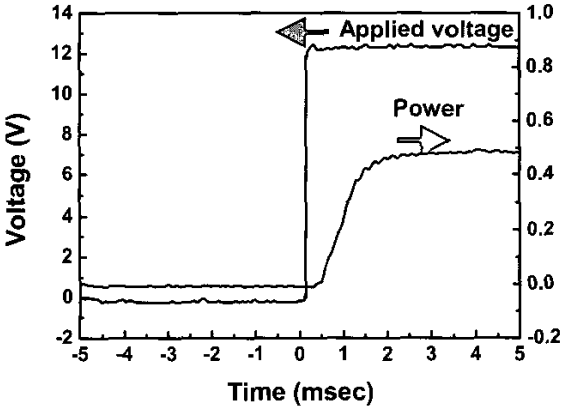

Figure 8. *Temporal response when the power is switched to the output port.*

REFERENCES

[1] L. Y. Lin, E. L. Goldstein, and R. W. Tkach, "Free-space micromachined optical switches for optical networking," IEEE J. Select. Topics Quantum Electronics: Special Issue on Microoptoelectro-mechanical Systems (MOEMS), vol. 5, pp. 4-9 (1999).

[2] A. Husain, "MEMS-based photonic switching in communications networks," in Proceeding of OFC 2001, WX1.

[3] R. Ryf, et al., "1296-port MEMS transparent optical crossconnect with 2.07Petabit/s switch capacity," in Proceedings of 2001 OFC postdeadline paper, PD28.

[4] D. T. Neilson, et al., "High-dynamic range channelized MEMS equalizing filter," in Proceedings of 2002 OFC, ThCC3, pp.586-588.

[5] J. E. Ford, V. A. Aksyuk, D. J. Bishop, and J. A. Walker, "Wavelength add-drop switching using tilting micromirrors," J. Lightwave Technology, vol.17, pp.904-11 (1999).

[6] D. M. Marom, et al., "Wavelength-selective 1x4 switch for 128 WDM channels at 50 GHz spacing," in Proceedings of 2002 OFC postdeadline paper, FB7.

[7] T. Ducellier, et al., "The MWS 1x4: a high performance wavelength switching building block," ECOC 2002, Session 2.3.1.

[8] S. Huang, J.C. Tsai, D. Hah, H, Toshiyoshi, and M. C. Wu, "Open-loop operation of MEMS WDM routers with analog micromirror array," in Proceedings of 2002 IEEE/LEOS Optical MEMS Conf, pp. 179-180.

[9] J. C. Tsai, S. Huang, D. Hah, and M. C. Wu, "Wavelength-selective $1xN^2$ switches with two-dimensional input/output fiber arrays," in Proceedings of CLEO 2003, CTuQ4.

[10] J. C. Tsai, S. Huang, D. Hah, and M. C. Wu, "Analog micromirror arrays with orthogonal scanning directions for wavelength-selective $1xN^2$ switches," in Proceedings of Transducers'03, pp.1776-1779.

[11] J. C. Tsai, S. Huang, D. Hah, and M. C. Wu, "$1xN^2$ wavelength-selective switch with telescope-magnified 2D input/output fiber collimator array," in Proceedings of 2003 IEEE/LEOS Optical MEMS Conf, pp. 45-46.

[12] M. Whitley, J. A. Hammer, Z. Hao, B. Wingfield, and L. Nelson, "A single two-axis micromachined tilt mirror and linear array," in Proceedings of SPIE Vol. 4985, pp.83-94.

[13] M. A. Helmbrecht, U. Srinivasan, C. Rembe, R. T. Howe, and R. S. Muller, "Micromirrors for adaptive-optics arrays," in Proceedings of Transducers'01, pp.1290-1293.

[14] J. H. Kim, H. K. Lee, B. I. Kim, J. W. Jeon, J. B. Yoon, and E. Yoon, "A high fill-factor micro-mirror stacked on a crossbar torsion spring for electrostatically-actuated two-axis operation in large-scale optical switch," in Proceedings of MEMS 2003, pp. 259-262.

[15] R. Sawada, J. Yamaguchi, E Higurashi, A. Shimizu, T. Yamamoto, N. Takeuchi, and Y. Uenishi, "Single Si crystal 1024ch MEMS mirror based on terraced electrodes and a high-aspect ratio torsion spring for 3-D cross-connect switch," in Proceedings of 2002 IEEE/LEOS Optical MEMS Conf, pp. 11-12.